

Zeitschrift: IABSE reports of the working commissions = Rapports des commissions de travail AIPC = IVBH Berichte der Arbeitskommissionen

Band: 16 (1974)

Artikel: Accuracy of simple design procedures for concrete columns

Autor: Oelhafen, Urs H.

DOI: <https://doi.org/10.5169/seals-15724>

Nutzungsbedingungen

Die ETH-Bibliothek ist die Anbieterin der digitalisierten Zeitschriften auf E-Periodica. Sie besitzt keine Urheberrechte an den Zeitschriften und ist nicht verantwortlich für deren Inhalte. Die Rechte liegen in der Regel bei den Herausgebern beziehungsweise den externen Rechteinhabern. Das Veröffentlichen von Bildern in Print- und Online-Publikationen sowie auf Social Media-Kanälen oder Webseiten ist nur mit vorheriger Genehmigung der Rechteinhaber erlaubt. [Mehr erfahren](#)

Conditions d'utilisation

L'ETH Library est le fournisseur des revues numérisées. Elle ne détient aucun droit d'auteur sur les revues et n'est pas responsable de leur contenu. En règle générale, les droits sont détenus par les éditeurs ou les détenteurs de droits externes. La reproduction d'images dans des publications imprimées ou en ligne ainsi que sur des canaux de médias sociaux ou des sites web n'est autorisée qu'avec l'accord préalable des détenteurs des droits. [En savoir plus](#)

Terms of use

The ETH Library is the provider of the digitised journals. It does not own any copyrights to the journals and is not responsible for their content. The rights usually lie with the publishers or the external rights holders. Publishing images in print and online publications, as well as on social media channels or websites, is only permitted with the prior consent of the rights holders. [Find out more](#)

Download PDF: 12.12.2025

ETH-Bibliothek Zürich, E-Periodica, <https://www.e-periodica.ch>

Accuracy of Simple Design Procedures for Concrete Columns

Précision des méthodes simples de dimensionnement des colonnes en béton

Über die Genauigkeit einfacher Bemessungsverfahren für Betonstützen

Urs H. OELHAFEN
Dr.sc.techn., Prof.
ITR Rapperswil Engineering College
Rapperswil, Switzerland

1. INTRODUCTION

Design methods for slender reinforced concrete columns based on allowable stresses have been proved to be inadequate. As a consequence of the non-linear relation between lateral deflections and cross-section forces these methods may claim safety levels which, in reality, are much smaller than the methods suggest. Thus, the prediction of ultimate load capacity is an essential point in most of the recent design procedures. Safety is vouched for by safety factors introduced where uncertainties are present: at the loads, at the strengths, at the stiffnesses, etc. The moment magnifier method as it is recommended in the ACI Building Code 318-71 (1) is an example of such a procedure. The accuracy of the moment magnifier method has been studied in recent investigations (2, 3) based on extensive computer analyses and comparisons with test results. It has been found that the accuracy of the method can be improved only within limits because the method does not distinguish properly between columns which might fail due to a material failure and those which might fail due to a stability failure.

This paper will outline ways of developing an alternative procedure which accounts for both types of failure by a step-by-step computation of the load-moment-curve (or load-deflection curve). Only the behavior of the hinged ended column bent in single curvature is considered. The investigation of the moment magnifier method (2, 3) will be quoted repeatedly because it is the basis of the method presented in this paper.

2. ANALYSIS OF SHORT TERM LOAD CAPACITY OF SLENDER COLUMNS

2.1 Method of Analysis

The computer analysis described briefly in this section was used to predict the strength and behavior of slender columns. The

results of design procedures were then compared to the results of this rigorous analysis. A more detailed description of the method of analysis is given in Refs. 2 and 4 .

Material Properties

1. Steel: idealized elastoplastic material
2. Concrete: stress-strain relationship
 - linear in the range $f'_t/E_c \leq \epsilon \leq 0$
 - quadratic parabola in the range $0 < \epsilon < 2f'_c/E_c$
 - perfectly plastic in the range $2f'_c/E_c \leq \epsilon \leq \epsilon_u$

Method of Analysis

1. The cross-section of a column subjected to uniaxial bending and compression is divided into a number of concrete and steel fibres parallel to the neutral axis.
2. The ultimate compression strain ϵ_u is divided into a number of segments which are selected as strain increments at the compressed edge of the cross-section.
3. By varying the strain distribution over the depth of the cross-section the sum of the internal forces (computed from the basic stress-strain relationships) is made equal to the external force P_i by means of a trial and error procedure.
4. By repeating of 3.) for all given values of P_i ($i=1,2,\dots, NP$) and all given values of ϵ_j ($j=1,2,\dots, NE$) the moment curvature relationship $M_{i,j}$, $\Phi_{i,j}$ results.
5. The influence of the concrete tensile zone will be included by subtracting a correction $\Delta\Phi$ from the computed curvature, Φ . The following corrections are applied:

$$M \leq M_0 : \quad \Delta\Phi = 0$$

$$M_0 < M < M_{cr} : \quad \Delta\Phi = \Delta\Phi_{cr} \frac{M - M_0}{M_{cr} - M_0}$$

$$M_{cr} \leq M : \quad \Delta\Phi = \Delta\Phi_{cr} \frac{M_{cr} - M_0}{M - M_0}$$

where: M_0 is the moment for zero strain at the tensile edge

M_{cr} is the cracking moment

$\Delta\Phi_{cr}$ is the difference between the curvature computed for the cracked cross-section and the curvature computed for the uncracked cross-section both evaluated for the moment $M = M_{cr}$.

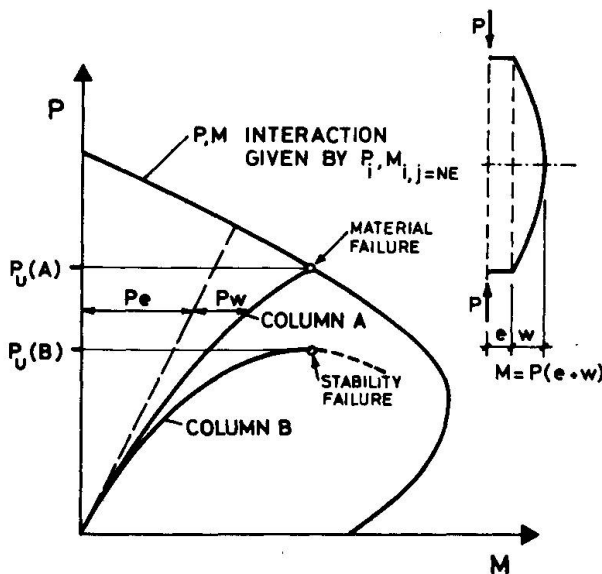


FIG. 1: BEHAVIOR OF SLENDER COLUMNS

6. The moment curvature relationships $M_{i,j}$, $\Phi_{i,j}$ are used in an iterative numerical integration procedure to determine the deflections, w , of the column subjected to P_i .
7. By repeating the computation of deflections for different values of P_i a load-moment relationship P, M representing the column behavior, can be found where M is the maximum moment at midheight given by $M = P(e + w)$. Failure is assumed to occur at the intersection of this P, M curve with the P, M interaction curve (material failure) or at the point on the P, M curve where dP/dM becomes zero (stability failure) as shown in Fig. 1. The interaction curve is given by P_i , $M_{i,j=NE}$ and follows for $j = NE$ from the moment curvature relationships.

2.2 Design of Computer Experiment

The variables listed in Table 1 were found to have the most effect on the column stiffness EI . To study the effects of these variables the eight values of each variable listed in Table 1 were chosen.

A fully factorial six factor experimental design with eight factor levels for each variable would call for 8^6 computer analyses or experiments. A Graeco-Latin square design allows to reduce this excessive number to 64 by an efficient combination of the variables. Each of the 64 cells in Table 2 represents one "computer experiment" and each of the first seven numbers in each cell represents the level of one variable listed in Table 1. For example, the combination 327458216 for cross-section shape B and slenderness ratio $l/h = 15$ means that the properties of this column were:

slenderness ratio l/h	= 15	←	3	2	7	4	5	8	2	1	6
cross-section shape B		←									
P_t (the 7th value in Table 1)	= 0.056	←									
d_c/h (the 4th value in Table 1)	= 0.125	←									
f'_c	= 6000 psi	←									
e/h	= 0.40	←									
φ_∞ (used in sustained load analysis only)	= 1.40	←									
											not used in the analysis

It is a feature of the Graeco-Latin square variable arrangement that each variable appears once with each value of every other variable (5). The Graeco-Latin square may therefore be considered as a representative sample of the fully factorial experiment. A residual sum of squares exists in the present case because the 8×8 Graeco-Latin square could contain nine instead of the six or seven variables used. The residual sum of squares in the Analysis of Variance allows an estimation of the total interaction of the variables.

TABLE 1
VARIABLES USED IN COMPUTER EXPERIMENT

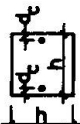
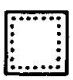

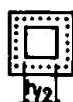




Order in Cell	Variable	Level of Variable							
		1	2	3	4	5	6	7	8
1.	Slenderness Ratio l/h	5	10	15	20	25	30	35	40
2.	Cross-Section Shape	A	B	C	D	E	F	G	H
									
3.	Reinforcement Ratio ρ_t	0.008	0.016	0.024	0.032	0.040	0.048	0.056	0.064
4.	Reinforcement Cover d_c/h	0.050	0.075	0.100	0.125	0.150	0.175	0.200	0.225
5.	Concrete Strength f'_c (psi)	2000	3000	4000	5000	6000	7000	8000	9000
6.	Load Eccentricity e/h	0.05	0.10	0.15	0.20	0.25	0.30	0.35	0.40
7.	Creep Coefficient ϕ (used in section 5)	0.8	1.4	2.0	2.6	3.2	3.8	4.4	5.0
Values of factors held constant:		$f_y = 60,000 \text{ psi}, E_s = 29.0 \times 10^6 \text{ psi},$ $f'_t = 6\sqrt{f'_c} \text{ (psi)}, E_c = 62726\sqrt{f'_c} \text{ (psi)}, \epsilon_u = 0.0035$							

TABLE 2
8 x 8 GRAECO-LATIN SQUARE EXPERIMENTAL DESIGN (REF.(5))

	Cross-Section Shapes (See Table 1)							
	A	B	C	D	E	F	G	H
Slenderness Ratio l/h	5	111111111	122546738	133268547	144387265	155734826	166475382	177823654
	10	212222222	221864375	237145863	246753148	258376514	264638751	273517486
	15	313333333	327458216	331786452	345162784	354215678	368524167	372671845
	20	414444444	426312857	435627318	441578623	453851762	462183576	478765231
	25	515555555	528137642	534872136	543426871	551643287	567361428	576284713
	30	616666666	624721583	638413725	642835417	657582341	661257834	675348172
	35	717777777	723685124	732354681	748241356	756128435	765816243	771432568
	40	818888888	825273461	836531274	847614532	852467153	863742615	874156327

3. ACCURACY OF THE MOMENT MAGNIFIER METHOD

3.1 Results of the ACI Moment Magnifier Method

The load capacity of the columns considered in the computer experiment has been computed from the moment magnifier method of the ACI Building Code 318-71. Following this method the maximum moment in a column with equal end-eccentricities can be calculated with sufficient accuracy for design purposes using Eqn. (1) (Ref. 7):

$$M_u = P_u e \frac{1}{1 - \frac{P_u}{P_{cr}}} \quad (1) \quad \text{where:} \quad P_{cr} = \frac{\pi^2 EI}{l^2} \quad (2)$$

EI has been assumed as suggested by ACI Equations (10-7) and (10-8). The ratios of theoretical to calculated ultimate loads were analyzed using an Analysis of Variance as shown in Table 3. F represents a statistical measure of the level of significance of the variance due to a certain variable. In the case considered the critical F value for the 1 % probability level is $F_{0.01} = 3.66$.

An F value greater than $F_{0.01}$ means that the probability is greater than 99 % that the variances are of a systematic character. It may be concluded that the variable in question will not be properly allowed for in the design procedure. This is the case for e/h if ACI Eqn. (10-7) is used and for P_t , e/h and l/h if ACI Eqn. (10-8) is used. The trend of the ratio P_u^{Th}/P_u^C is shown in Fig. 2. Each point in Fig. 2 represents the mean of eight columns having the same factor level of the variable considered. A frequency distribution of P_u^{Th}/P_u^C is shown in Fig. 3.

3.2 Evaluation of Improved EI Equations

The columns analyzed in the computer experiment were used to derive more reliable EI Equations. From the results P_u and M_u for each column one stiffness value EI can be found by substituting P_u and M_u into Eqn. (1) and solving Eqns. (1) and (2) for EI:

$$EI = \frac{P_u M_u}{M_u - e P_u} \cdot \frac{l^2}{\pi^2} \quad (3)$$

In the case of a stability failure the ultimate moment was taken from the point on the interaction diagram corresponding to the computed ultimate load. The population of these EI values from all the columns analyzed represents the basis for an evaluation of simplified EI equations containing the most significant variables.

From a stepwise multiple regression analysis incorporating the three most important variable-combinations the following regression equation resulted:

$$EI = E_c I_g \left(0.205 + 0.000622 \frac{l}{e} + 0.731 \frac{E_s I_s}{E_c I_g} \right) \quad (4)$$

For Eqn. (4) the multiple correlation coefficient is 0.908. Only minor improvements could be achieved by taking further variables into the regression. The Analysis of Variance (Table 3) shows a much smaller total sum of squares and a more adequate consideration of all the variables as can be seen from the F-values.

Equation (4) was considered impractical in design practice because the term l/e leads to an overestimation of EI for very small eccentricities and because the same term is not clearly defined for unequal end-eccentricities. Finally, an EI equation well suited for design practice was found by a number of simplifications (2):

$$EI = E_c I_g \left(0.25 + \frac{E_s}{E_c} P_t \right) \quad (5)$$

For this equation the mean ratio of theoretical to calculated ultimate load was 1.043, the coefficient of variation was 18.7 %. The lower coefficient of variation indicates a better level of prediction and a better fit into the data than ACI Equations (10-7) and (10-8) but the eccentricity ratio e/h has still a significant effect on the ratio P_u^{Th}/P_u^C . The frequency distribution of P_u^{Th}/P_u^C is shown in Fig. 3.

It is improbable that the moment magnifier method can be improved substantially by further developments of stiffness formulas in a manner similar to the one described above. A major portion of the variances are attributable to the fact that stability failures are practically reduced to material failures. Thus, it is the aim of the following section to develop a procedure which takes proper account of both types of failure.

4. STEP-BY-STEP ANALYSIS PROCEDURE FOR COLUMN DESIGN

4.1 A Simplified Step-by-Step Analysis Procedure

A design procedure which accounts for the influence of the internal forces on the column stiffness was found to produce much better results. The simplified strain-controlled procedure described in this section proved to be efficient and able to cover both types of failure.

TABLE 3

MOMENT MAGNIFIER METHOD

ANALYSIS OF VARIANCE FOR P_u^{Th}/P_u^C (THEORETICAL COMPUTED ULTIMATE LOADS = $\frac{P_u^{Th}}{P_u^C}$)

Source of Variation	Degrees of Freedom	ACI Eqn.(10-7)			ACI Eqn.(10-8)			Eqn.(4)		
		Sums of Squares	Mean Square	F	Sums of Squares	Mean Square	F	Sums of Squares	Mean Square	F
Shapes	7	0.287	0.0410	1.26	0.396	0.0566	1.46	0.0712	0.0102	1.18
l/h	7	0.444	0.0635	1.95	1.153	0.1647	<u>4.26</u>	0.0367	0.0052	0.61
P_t	7	0.323	0.0461	1.42	1.913	0.2733	<u>7.06</u>	0.0454	0.0065	0.75
d_c/h	7	0.174	0.0248	0.76	0.303	0.0433	1.12	0.0359	0.0051	0.59
f'_c	7	0.309	0.0442	1.36	0.323	0.0462	1.19	0.0525	0.0075	0.87
e/h	7	1.482	0.2117	<u>6.52</u>	1.888	0.2697	<u>6.97</u>	0.1401	0.0200	2.32
Residuals	21	0.682	0.0325		0.813	0.0387		0.1811	0.0086	
Total	63	3.701			6.789			0.5629		
<u>Total Sample</u>										
Mean		1.099			1.168			1.001		
Coef. of Variation		22.0 %			28.1 %			9.4 %		

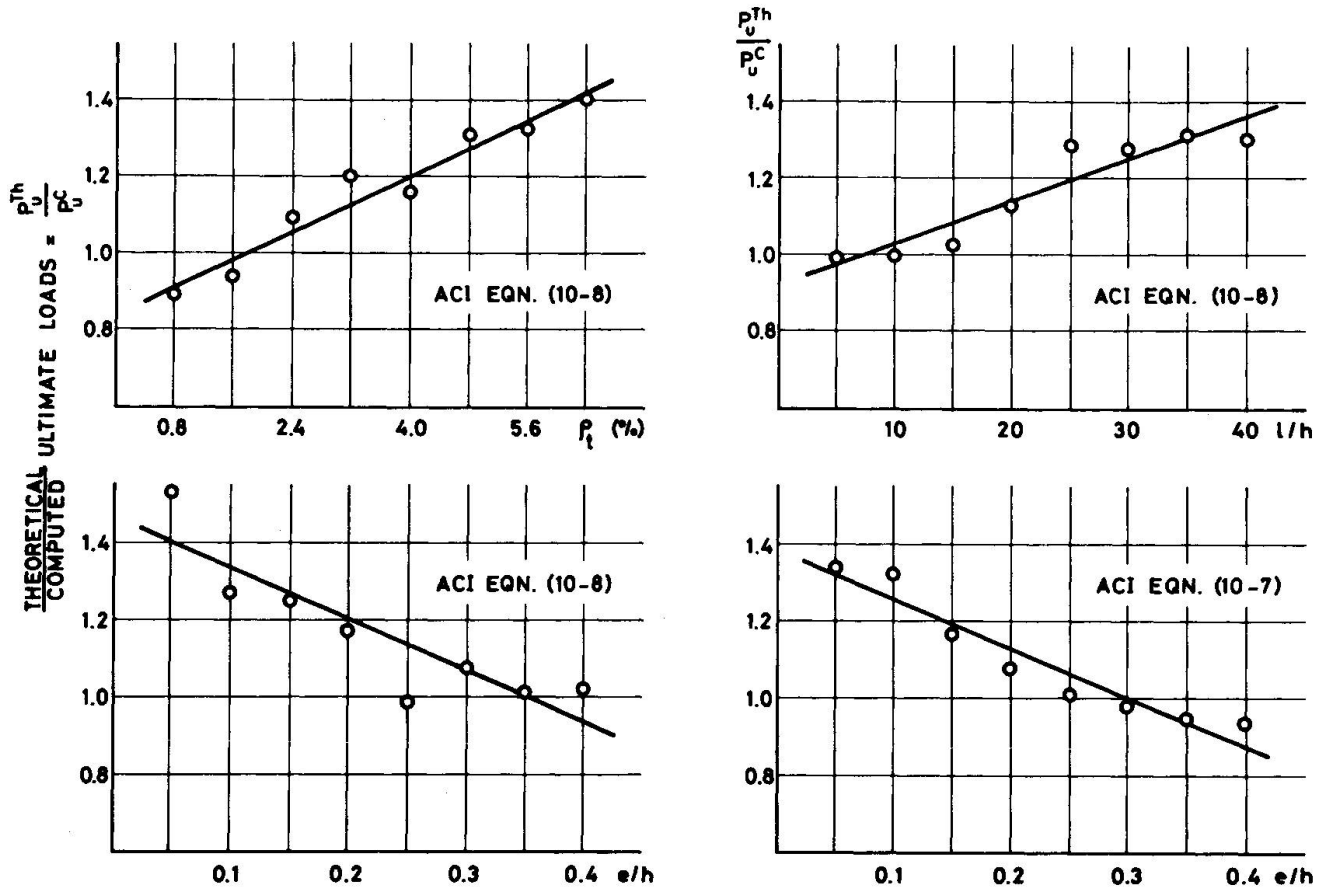


FIG. 2: SIGNIFICANT EFFECTS OF VARIABLES

In the critical cross-section a strain ϵ_1 at the compressed edge is chosen and by assuming a strain distribution over the depth of the cross-section the axial load P , the internal moment M_i and the external moment $M_e = P(e+w)$ may be computed. The strain at the compressed edge is held constant and the strain distribution is varied until M_i and M_e are made equal. Usually this can be achieved by assuming two or three strain distributions as a design example will show. In the next step the procedure described is repeated for an increased strain ϵ_1 . Very few steps are required to allow an accurate prediction of the ultimate load capacity.

The following example of a slender column subjected to short-term loading may illustrate the method. Table 4 contains the data of a column tested in a short-term loading experiment (4,17). The broken line in Fig. 5 shows the experimental relationship between load and moment at midheight.

To start the computation the values $\epsilon_1/\epsilon_0 = 0.25$ and $\epsilon_2/\epsilon_1 = 0.20$ are assumed. For these values the diagrams in Fig. 4 yield the following coefficients:

$$\begin{aligned} k_c &= 0.280 & , & & k_y &= 0.105 \\ k_s &= 0.334 & , & & k'_s &= 0.865 \end{aligned}$$

Eqn. (6) gives the force P associated with the assumed strain distribution:

$$P = \int_{A_c} \sigma_c dA_c + \sigma'_s A'_s + \sigma_s A_s \quad (6)$$

and in the case of the rectangular cross-section considered with $A'_s = A_s$:

$$\begin{aligned} P &= P_c + P'_s + P_s \\ &= k_c \cdot P_o + (k'_s + k_s) \cdot \epsilon_1 \cdot E_s \cdot A_s \\ &= 0.28 \cdot 86.25 + (0.334 + 0.865) \cdot 0.0005 \cdot 2100 \cdot 3.14 = 28.1 \text{ Mp} \end{aligned} \quad (6a)$$

The restrictions

$$\epsilon'_s = k'_s \epsilon_1 \leq f_y / E_s$$

and $|k_s| = |k_s| \epsilon_1 \leq f_y / E_s$ are fulfilled.

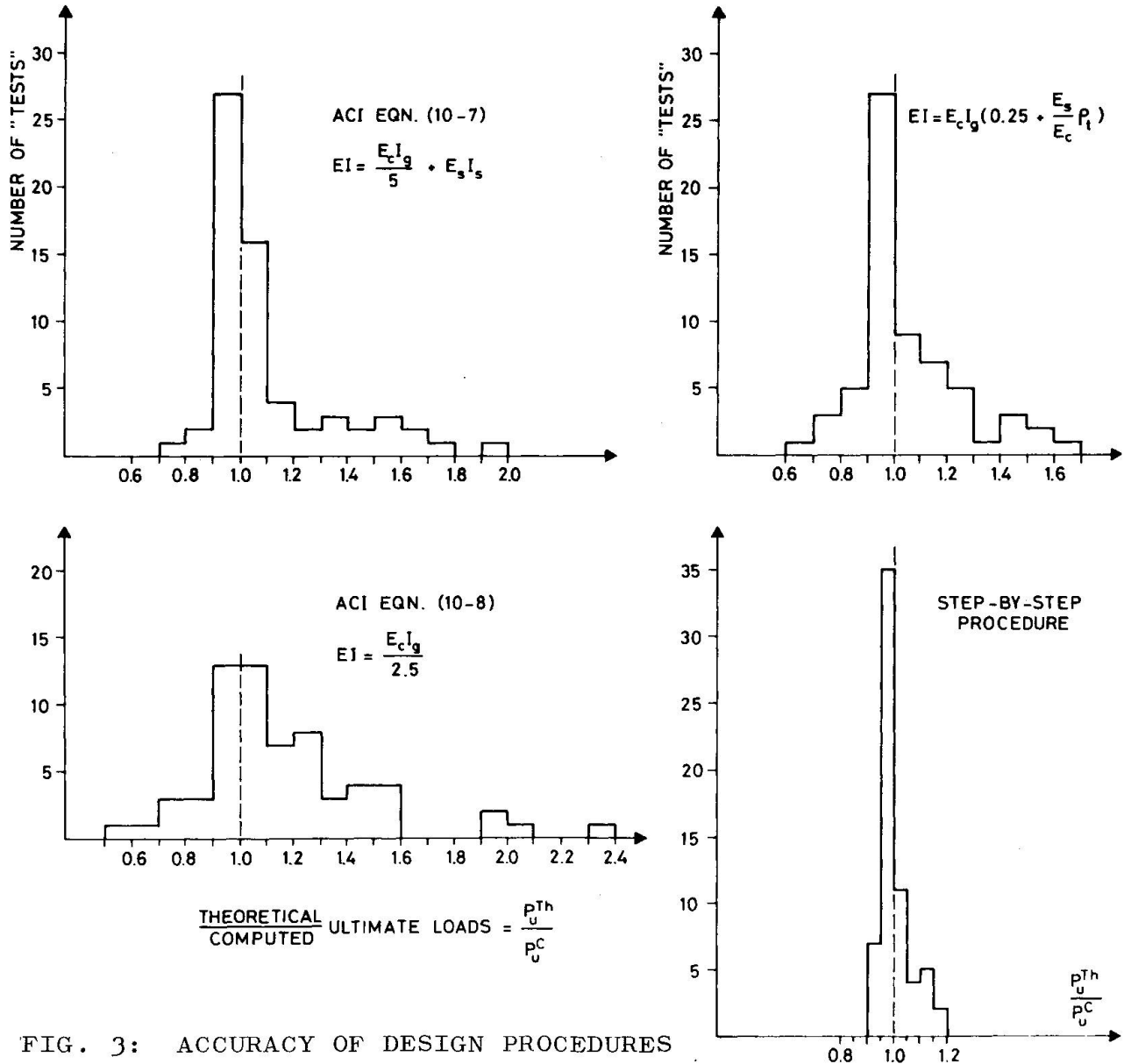
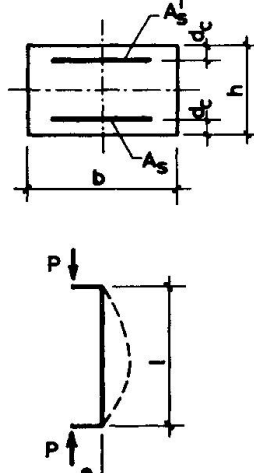
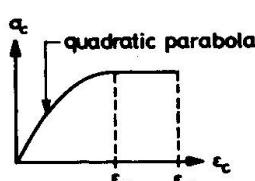


FIG. 3: ACCURACY OF DESIGN PROCEDURES

TABLE 4
COLUMN DATA USED IN DESIGN EXAMPLE

Column Test No.41; Refs.(4),(17); Short-Term Loading	
Cross-Section and Dimensions	Material Properties and Design Data
 <p> $b = 25.0 \text{ cm}$ $h = 15.0 \text{ cm}$ $d_c = 2.5 \text{ cm}$ $A_s = 3.14 \text{ cm}^2$ $A'_s = 3.14 \text{ cm}^2$ $l = 432.6 \text{ cm}$ $e = 0.5 \text{ cm}$ </p>	<p>Concrete: $f'_c = 0.75 f'_{\text{cube } 28} = 230 \text{ kp/cm}^2$ $E_c = 229'000 \text{ kp/cm}^2$ $P_o = f'_c b h = 86.25 \text{ Mp}$ $\epsilon_o = \frac{2 f'_c}{E_c} = 2.0 \cdot 10^{-3}$ $\epsilon_u = 3.5 \cdot 10^{-3}$</p> <p>Steel: $f_y = 4'600 \text{ kp/cm}^2$ $E_s = 2.1 \cdot 10^6 \text{ kp/cm}^2$ $P_{sy} = P'_{sy} = f_y A_s = 14.45 \text{ Mp}$</p> 

Eqn. (7) gives the moment M_i associated with the assumed strain distribution:

$$M_i = \int_{A_c} \sigma_c y_c dA_c + (\sigma'_s A'_s - \sigma_s A_s) y_s \quad (7)$$

and for the rectangular cross-section:

$$\begin{aligned} M_i &= P_c \cdot k_y \cdot h + (P'_s - P_s) \cdot y_s \\ &= 24.15 \cdot 0.105 \cdot 15 + (2.85 - 1.10) \cdot 5 = 46.8 \text{ Mpcm} \end{aligned} \quad (7a)$$

EI and P_{cr} may be computed from M_i :

$$EI = \frac{M_i h}{\epsilon_1 - \epsilon_2} \quad (8) \quad \text{and} \quad P_{cr} = \frac{\pi^2 EI}{l^2} = \pi^2 \frac{h}{l^2} \frac{M_i}{(\epsilon_1 - \epsilon_2)} \quad (9)$$

In the example: $P_{cr} = 7.91 \cdot 10^{-4} \frac{46.8}{(0.5 - 0.1) \cdot 10^{-3}} = 92.5 \text{ Mp}$

By Eqn. (8) the stiffness EI is computed from moment and curvature at the critical cross-section. Idealized, EI is assumed to be constant over the entire column length. As a further idealization the influence of the tensile zone is neglected.

Eqn. (10) gives the external moment M_e somewhat more accurate than Eqn. (1) as section 4.2 will show

$$M_e = P e \frac{1 + 0.234 \frac{P}{P_{cr}}}{1 - \frac{P}{P_{cr}}} \quad (10)$$

Example: $M_e = 28.1 \cdot 0.5 \frac{1 + 0.234 \frac{28.1}{92.6}}{1 - \frac{28.1}{92.6}} = 21.6 \text{ Mpcm}$

Compared to the internal moment, M_i , the calculation yields a smaller value for the external moment, M_e . A smaller value of M_i and a larger value of M_e is obtained by an increase of the axial load; this can be achieved by an increase of the strain ϵ_2 if ϵ_1 is held constant. For $\epsilon_2/\epsilon_1 = 0.5$ the resulting moments $M_i = 23.5 \text{ Mpcm}$ and $M_e = 35.2 \text{ Mpcm}$ are listed in the second row of Table 5. Now, M_i is the smaller and M_e the larger value.

In the P,M diagram of Fig. 5 values of M_i and M_e belonging to the axial load values $P=28.1 \text{ Mp}$ and $P=34.3 \text{ Mp}$ are entered. The P, M_i curve and the P, M_e curve are approximated by two straight lines within the load range.

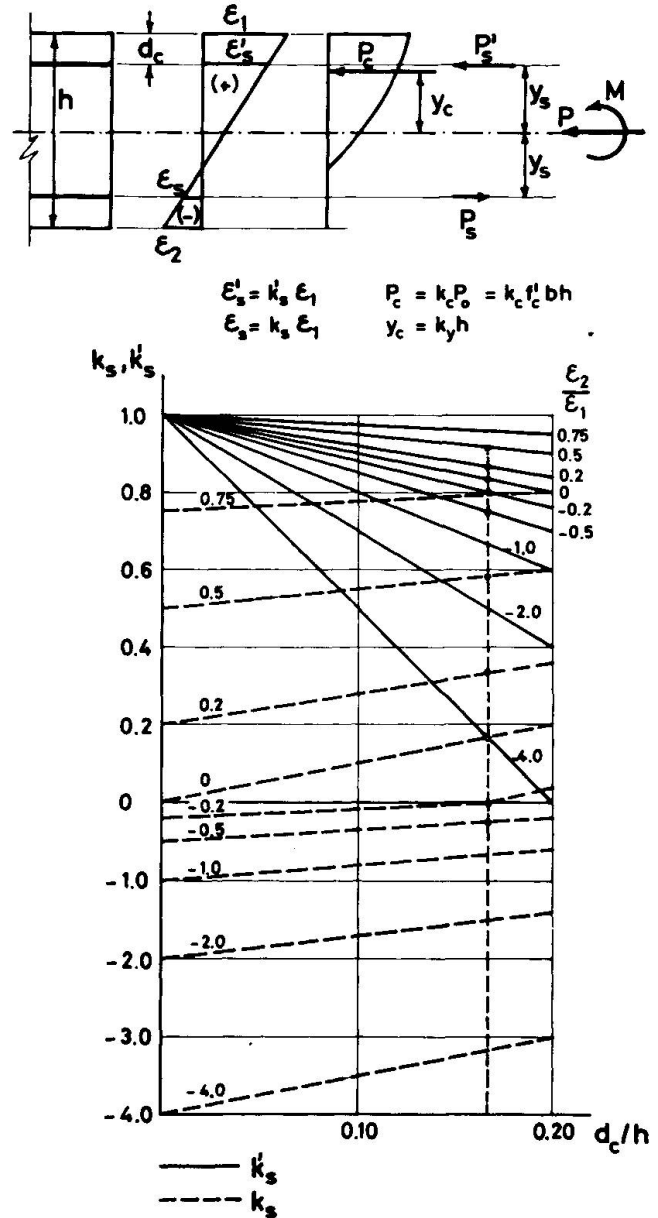
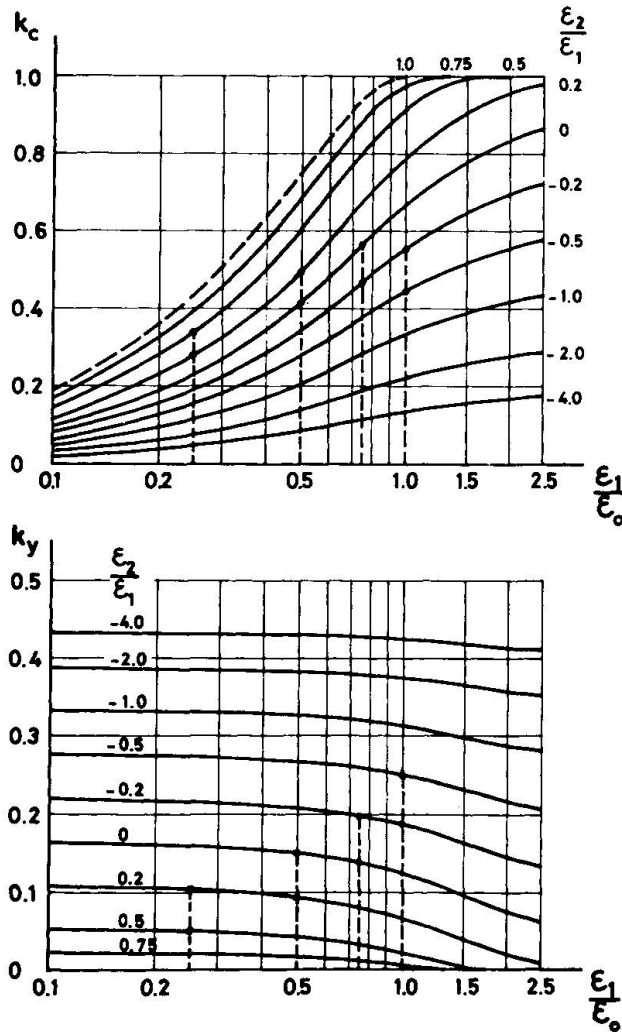


FIG. 4: COMPUTATION OF INTERNAL FORCES;
COEFFICIENTS FOR RECTANGULAR CROSS-SECTIONS

The first point of the P,M relationship follows from the intersection of these two straight lines.

In the next step the strain ϵ_1 is increased to $\epsilon_1 = 0.5 \epsilon_0$ and the computational procedure described above is repeated. As a result a second point of the P,M relationship is found. With two more values of ϵ_1 the P,M curve can be plotted sufficiently accurate as Fig. 5 indicates.

TABLE 5
COMPUTATION OF P , M_i AND M_e

$\frac{\epsilon_1}{\epsilon_0}$	$\frac{\epsilon_2}{\epsilon_1}$	P Eqn. (6a)	M_i Eqn. (7a)	P_{cr} Eqn. (9)	M_e Eqn. (10)
0.25	0.2	28.1	46.8	92.5	21.6
0.25	0.5	34.3	23.5	74.5	35.2
0.50	0.0	43.3	104.5	82.6	50.9
0.50	0.2	50.8	77.3	76.5	87.4
0.75	-0.2	48.5	160.0	70.3	90.5
0.75	0.0	58.8	134.2	70.8	207.7
1.00	-0.5	45.1	210.6	55.3	146.2
1.00	-0.2	58.5	187.3	61.5	731.3

The resulting ultimate load capacity is $P_u^C = 53.3$ Mp. The corresponding value measured in the experiment was $P_u^{Test} = 52.5$ Mp. It is interesting to compare this result with the moment magnifier method described previously using different EI equations:

$$\text{Ratio of } P_u^{Test}/P_u^C$$

Step-by-Step Procedure: 0.985
EI from ACI Eqn. (10-7): 1.64
EI from ACI Eqn. (10-8): 1.64
EI from Eqn. (4): 0.83
EI from Eqn. (5): 1.64

As Figures 3 and 5 show the step-by-step procedure is in any case a much better approach to the column behavior than the moment magnifier method.

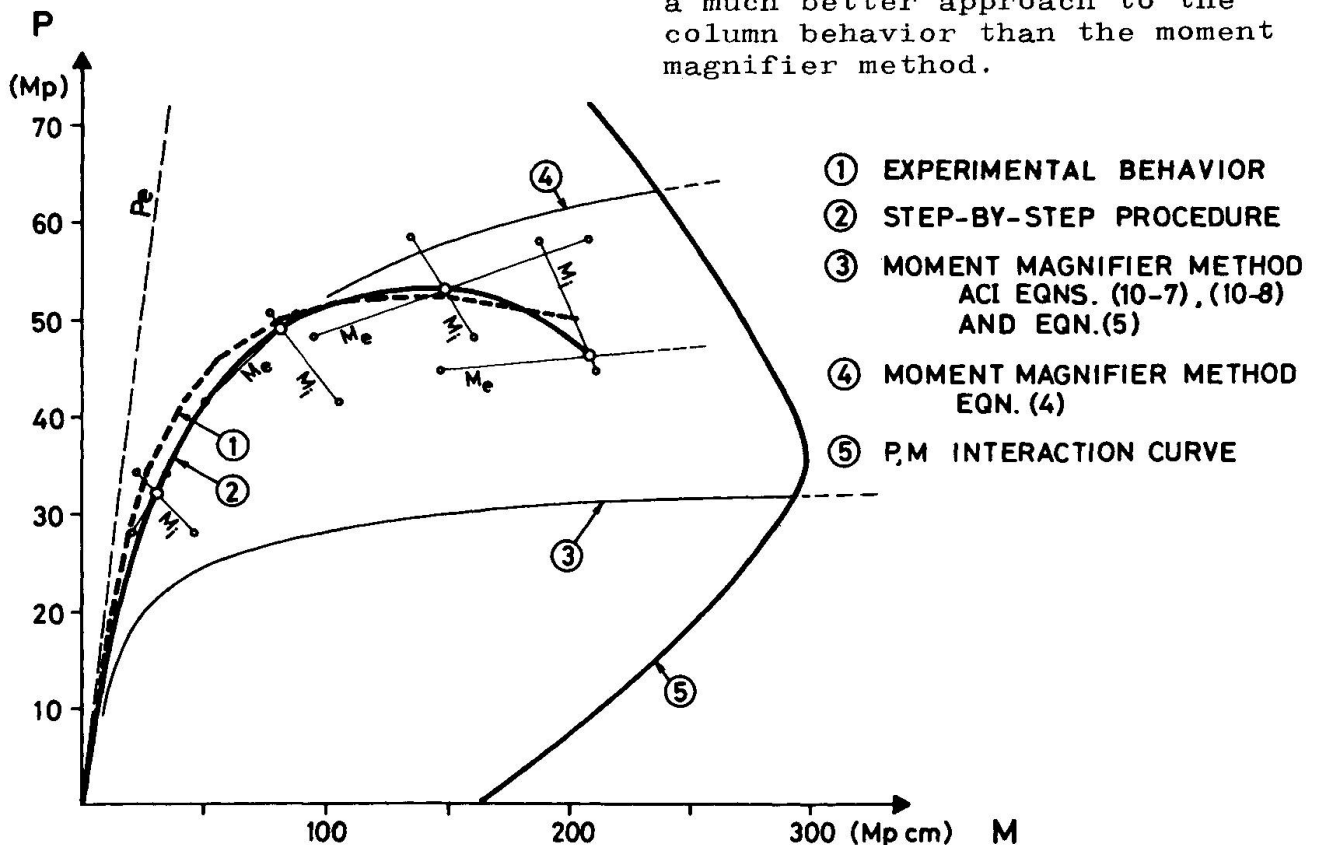


FIG. 5: EXPERIMENTAL BEHAVIOR OF A SLENDER COLUMN AND COMPUTATIONAL APPROACH

The use of a programmable desk calculator makes the method described more efficient; because of an automatic trial and error procedure the results are also more accurate. A program for general cross-section shapes and positions of reinforcement developed on a HP 9810A desk calculator requires about 1000 program steps and less than 50 data storage registers.

4.2 Comparison of the Analysis Procedure with Computer Tests

The analysis procedure described in the preceding section has been used to compute the ultimate load capacity of the 64 columns investigated in the computer experiment. In addition to Eqn. (10) the following equations have been used to compute the moment M_e :

$$M_e = P_e \frac{1}{1 - \frac{P}{P_{cr}}} \quad (11)$$

and
$$M_e = \frac{Pe_2}{\sin \lambda l} \sqrt{\alpha^2 - 2\alpha \cos \lambda l + 1} \quad (12)$$

$$\lambda = \sqrt{\frac{P}{EI}} \quad , \quad \alpha = \frac{e_1}{e_2} \quad : \text{ratio of end-eccentricities}$$

-1 < α < 1 (in the case considered: $\alpha = 1$)

Eqn. (11) represents a simple approximative solution of the maximum moment in an elastic beam-column bent in single curvature with equal end-eccentricities. More accurate for that type of column is Eqn. (10). Finally, Eqn. (12) represents the solution of the differential equation including the case of unequal end-eccentricities.

TABLE 6
STEP-BY-STEP ANALYSIS PROCEDURE

ANALYSIS OF VARIANCE FOR P_u^{Th}/P_u^C ($\frac{\text{THEORETICAL}}{\text{COMPUTED}}$ ULTIMATE LOADS = $\frac{P_u^{Th}}{P_u^C}$)

Source of Variation	Degrees of Freedom	Eqn. (10)			Eqn. (11)			Eqn. (12)		
		Sums of Squares	Mean Square	F	Sums of Squares	Mean Square	F	Sums of Squares	Mean Square	F
Shapes	7	0.0171	0.00244	1.40	0.0091	0.00130	1.14	0.0176	0.00251	1.40
l/h	7	0.0656	0.00937	<u>5.39</u>	0.0215	0.00308	2.69	0.0743	0.01061	<u>5.90</u>
P_t	7	0.0432	0.00617	3.55	0.0220	0.00314	2.74	0.0446	0.00638	3.55
d_c/h	7	0.0055	0.00079	0.45	0.0050	0.00072	0.63	0.0056	0.00080	0.45
f'_c	7	0.0093	0.00132	0.76	0.0052	0.00075	0.65	0.0098	0.00140	0.78
e/h	7	0.0272	0.00388	2.23	0.0171	0.00245	2.14	0.0284	0.00405	2.25
Residuals	21	0.0365	0.00174		0.0240	0.00114		0.0378	0.00180	
Total	63	0.2044			0.1039			0.2181		
<u>Total Sample</u>										
Mean		1.005			0.958			1.008		
Coef. of Variation		5.7 %			4.2 %			5.8 %		

Eqn. (11) was found to show the smallest variances (Table 6). All variables may be considered as adequately taken into account because all F-values are smaller than $F_{0.01}$. However, the low mean of 0.958 indicates a distinct tendency to overestimate the ultimate load capacity. The variances are larger for Eqns. (10) and (12) and the influence of the slenderness is on a significant level. As a general trend the load capacity of a slender column tends to be underestimated. Thus, the design is slightly more conservative for slender columns; a fact which may not be undesirable. Preference should be given to Eqns. (10) and (12) because the mean is much more clearly illustrated by these equations than by Eqn. (11) (Table 6).

The evaluation of ϵ_u is difficult, since ϵ_u depends on a wide range of factors (Ref. 6). As an alternative approach, Ref. 6 suggests to allow the stress-strain curve to extend indefinitely and to identify failure when the rate of increase of applied load is zero. The results of a computation based on this assumption was only unessentially different. The mean of P_u^{Th}/P_u^C was 0.996, the coefficient of variation was 6.6 %, maximum and minimum values were 1.179 and 0.831. Eqn. (10) was used to compute M_e . About 30 % of the columns investigated were affected by ϵ_u , all other columns failed before $\epsilon_u = 0.0035$ was reached.

TABLE 7

COMPARISON OF DESIGN METHODS WITH COLUMN TESTS

Investigator	Reference	No. of Tests	Ratio of p_u^{Test}/p_u^C							
			Moment Magnifier Method						Step-by-Step Method	
			ACI Eqn. (10-7)		EI from ACI Eqn. (10-8)		Eqn. (5)		M_e from Eqn. (10)	
			Mean	Coef. of Var.	Mean	Coef. of Var.	Mean	Coef. of Var.	Mean	Coef. of Var.
				%		%		%		%
Thomas	9	12	1.584	27.5	1.424	31.7	1.163	24.0	0.917	16.5
Ernst, Hromadik, Riveland	12	7	1.092	24.5	1.007	20.9	1.064	23.4	0.989	15.3
Goyal, Jackson	19	26	1.015	8.0	1.035	7.6	1.012	7.0	0.942	3.6
Ferguson, Chang	14	6	1.210	22.2	1.139	23.1	1.192	23.2	0.849	10.0
Drysdale, Huggins (Rectangular)	18	4	1.171	2.5	1.470	22.0	1.283	2.4	1.057	2.8
Drysdale, Huggins (Diamond)	18	10	1.212	4.9	1.155	5.4	1.307	5.0	1.084	4.5
Baumann	8	13	1.212	28.8	1.079	22.7	1.215	26.1	1.040	21.6
Ramboll	11	29	1.208	22.8	1.089	16.2	1.148	19.4	1.202	13.7
Hanson, Rosenstrom	10	3	1.664	5.9	1.202	6.4	1.511	4.5	1.119	6.1
Kordina	20	4	1.199	13.1	1.030	12.6	1.199	13.1	1.019	9.9
Thürlimann	17	6	1.105	27.2	1.036	25.1	1.084	26.5	0.805	9.1
Gaede (Rectangular)	13	8	0.884	13.0	0.787	10.7	0.888	13.2	0.897	6.4
Gaede (Diamond)	15	11	1.093	11.1	0.986	10.0	1.093	11.1	1.071	13.5
Robinson, Modjabi (Channel)	16	4	1.388	14.8	1.671	16.0	1.526	15.0	1.138	18.8
Tal, Chistiakov	21	60	1.253	22.6	1.222	16.6	1.345	18.2	1.075	12.4
Mehmel	22	14	-	-	-	-	-	-	0.952	10.3
Overall		217	1.202	24.1	1.162	22.9	1.202	21.2	1.035	15.6

4.3 Comparison of the Analysis Procedure with Tests

The analysis procedure described in section 4.1 has been used to compute the ultimate load capacity of 217 columns tested in short-term tests in 16 investigations (Refs. 8-22). The comparisons have been limited to hinged columns bent in symmetrical single curvature. All but 25 of the columns were rectangular. The same assumptions made in Ref. 2 concerning concrete strength have been used in the present investigation. The external moment M_e has been computed from Eqn. (10).

The results are presented in Fig. 6 and Table 7. The mean, the coefficient of variation and the frequency distribution of the proposed procedure are distinctly improved compared to the results of the moment magnifier method reported in Ref. 2.

5. EFFECT OF LOAD DURATION

5.1 Sustained Load Behavior of Columns

The knowledge of the effect of sustained loads on the strength of slender columns has been improved in the past two decades by experiments (Refs. 13, 15, 17, 18, 19, 20) and analyses of the problem (Refs. 3, 4, 18, 19, 20, 23, 24).

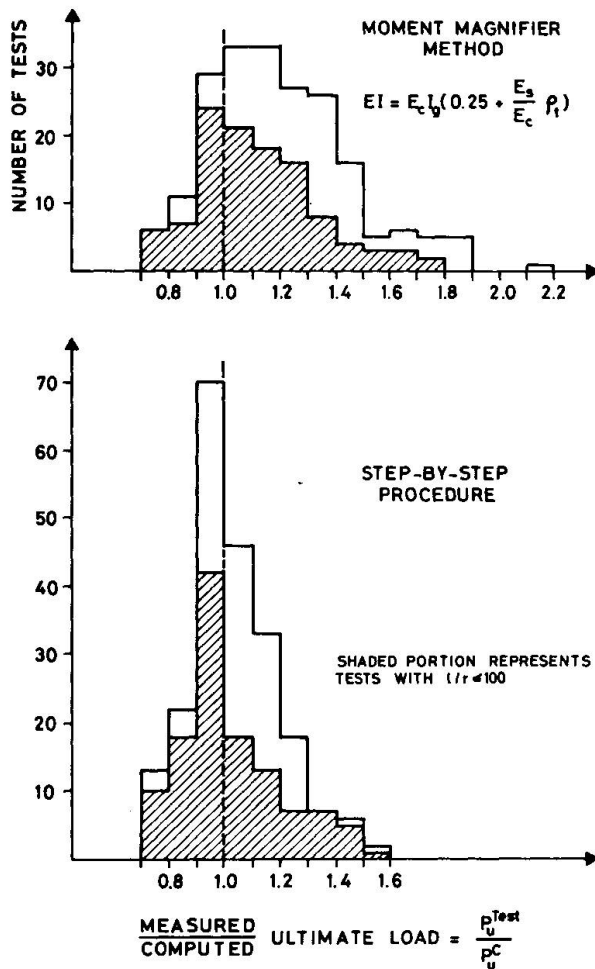


FIG. 6: COMPARISON OF DESIGN PROCEDURES WITH TESTS

In Ref. 3 an incremental rate-of-creep analysis has been developed and used to generate data for a statistical evaluation of the effect of creep on the stiffness, EI . Each of the 64 columns investigated in the computer experiment described in section 2.2 was analyzed to determine the critical sustained load capacity and the remaining short-term load capacities after the column had been subjected to sustained loads. An average of 7 or 8 sustained load levels P_i was chosen for each column and the resulting total population included 482 values of $P_{u\infty,i}$ and $M_{u\infty,i}$.

The behavior of a slender column under short-term and sustained loads is shown qualitatively in Fig. 7. Curve (A) shows the instantaneous short-term behavior expressed in terms of load and moment at midheight. Curve (B) shows the behavior of a column loaded up to failure after being subjected to a sustained load P_i during a period of time, t . Failure is assumed to occur at the intersection with a P, M -interaction curve (\bar{B}) computed with a slightly increased

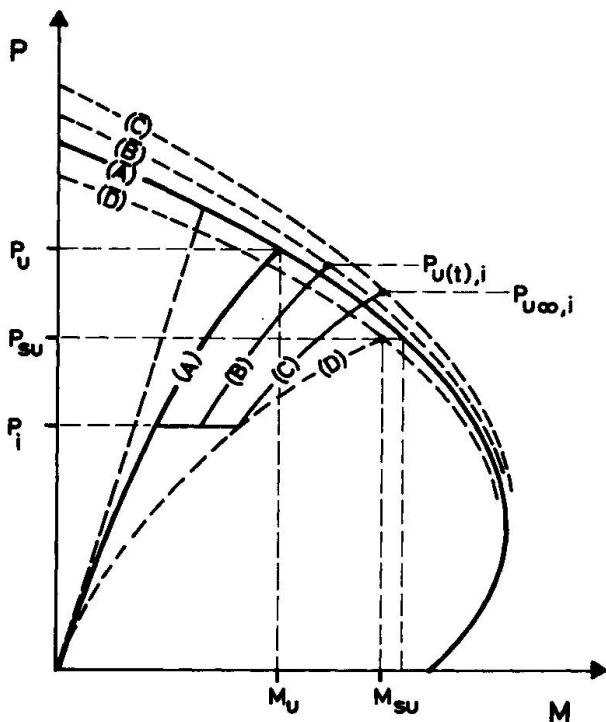


FIG. 7: BEHAVIOR OF A COLUMN UNDER SHORT TERM AND SUSTAINED LOADS

tained loads greater than P_{su} the column will fail under the sustained load (4, 23).

It is important to note that the design of a column subjected to sustained loads requires two separate safety checks. The column would first be proportioned for the total design (ultimate) load. In a second step the designer ought to check whether the column would fail during the sustained load period when subjected to sustained loads only.

5.2 Analysis of Sustained Load Capacity of Columns

A more complete description of the method of analysis is given in Ref. 3. The assumptions made for the material behavior and for the step-by-step Rate-of-Creep analysis are summarized briefly in the following.

The creep function $\varphi(t)$ is defined as the ratio between creep strain and initial strain:

$$\varphi(t) = \frac{\epsilon_{CR}(t)}{\epsilon} \quad (13)$$

ϵ is given by the equation of the short-term stress-strain curve:

$$\epsilon = \frac{2f'_c}{E_c} \left(1 - \sqrt{1 - \frac{f_c}{f'_c}} \right) \quad (14)$$

The function $\varphi(t)$ has been derived from tests on plain concrete specimens subjected to different load levels (Refs. 3, 4); it was found that the stress dependency of the creep function at

concrete strength due to maturing. The basic P,M-interaction curve (\bar{A}) is computed with the initial (28 days age) concrete strength. Curve (C) shows the behavior of a column loaded up to failure after the total amount of creep possible under the sustained load P_i has occurred. Curve (D) represents the maximum possible increase in the moment at failure section due to creep. The intersection of this limiting curve and the interaction curve (\bar{D}) yields the critical sustained load P_{su} which is the lowest load that can cause a creep failure. Because the strength of concrete tends to decrease under sustained high stresses (26) interaction curve (\bar{D}) is situated slightly lower than interaction curve (\bar{A}).

For sustained loads less than P_{su} the column load can be increased to failure at time $t = \infty$ as shown by curve (C). For sus-

tained loads greater than P_{su} the column will fail under the sus-

any time t can be expressed by

$$\varphi(t) = c_1(t) + c_2(t) \frac{f_c}{f'_c} \quad (15)$$

where

$$c_{1,2}(t) = \bar{c}_{1,2} [1 - \exp(-\kappa_{1,2} t^{\delta_{1,2}})] \quad (16)$$

$$\bar{c}_1 = \frac{[\varphi(\infty, 0.40) - 0.8]}{3} \quad (17)$$

$$\bar{c}_2 = 2.5 [\varphi(\infty, 0.40) - \bar{c}_1] \quad (18)$$

In these expressions $\varphi(\infty, 0.40)$ refers to time $t=\infty$ and $f_c/f'_c=0.40$ and is taken equal to the value of φ given by the CEB Recommendations (25).

Preliminary studies on columns with an equal amount of reinforcement on both faces have shown that the effect of shrinkage was insignificant and consequently it has not been considered in this study.

The increase in the strength of the concrete due to maturing was included and conservatively assumed to be 1.10 times the 28 day strength at time infinity. The decrease in concrete strength in the presence of high sustained stresses was assumed to be 20 percent of the short time strength (26).

In 2.1 the computation of the moment-curvature relationship $M_{i,j}$, $\Phi_{i,j}$ has been described. To include the effect of creep, this relationship had to be expanded to $M_{i,j}$, $\Phi_{i,j,k}$. The index k stands for time, where $k=1$ indicates values for the short-term loading situation so far referred to as $\Phi_{i,j}$. The values $\Phi_{i,j,k}$ for $k=2,3,\dots,NT$ are computed by a Rate-of-Creep Method considering the viscoelastic behavior of any single fibre in the cross-section and using time as a discrete variable (3). The time dependent deflections of a column subjected to a sustained load were computed by the Rate-of-Creep Method making use of the $M_{i,j}$, $\Phi_{i,j,k}$ relationship.

5.3 Design Methods Accounting for the Effect of Creep

As discussed in Ref. 28 for design purposes there are essentially three major methods of accounting for sustained load effects. These are the Reduced E-Modulus Method used in the ACI Code (1), the Dischinger Method (27) and the Sustained Load Eccentricity Method (29). For these methods creep parameters have been derived statistically from computer experiments similar to the evaluation of EI equations discussed in section 3.2 (Ref. 3).

The 1971 ACI Code includes the effect of creep by reducing the flexural stiffness to $EI_R = EI/(1 + \beta_d)$. The load transfer to the reinforcement due to creep may cause premature yielding of the compression reinforcement and for this reason both the concrete and the steel terms in the ACI equations were reduced. With the trend to higher steel percentages this procedure was found to be excessively conservative (3). Accordingly Eqns. (19) and (20) have been used in Ref. 3 to define the reduced modulus:

$$EI_R = E_c I_g \left(\frac{0.25}{\beta} + \frac{E_s}{E_c} \rho_t \right) \quad (19)$$

or

$$EI_R = \frac{E_c I_g}{5\beta} + E_s I_s \quad (20)$$

Eqn. (19) or Eqn. (20) may be substituted into Eqn. (21) to obtain the magnified moment

$$M(t) = \frac{Pe}{1 - \frac{Pl^2}{\pi^2 EI_R}} \quad (21)$$

Eqn. (21) can be solved for EI_R and β using the values of $P_{u\infty,i}$ and $M_{u\infty,i}$. By computing β for all the columns analyzed in the computer experiment, a population of 482 β values is created which can be used to derive design equations for β by stepwise multiple regression analysis. The resulting linear regression equation was

$$\beta = 1.016 - 11.45 \rho_t + 0.107 \varphi_\infty - 0.0126 \frac{l}{h} + 0.318 \beta_P^2 \geq 1.0 \quad (22)$$

The variables included in Eqn. (22) are the most significant of 13 variables and variable combinations considered. For design practice Eqn. (22) then has been simplified to Eqn. (23)

$$\beta = 0.9 + 0.5 \beta_P^2 - 12 \rho_t \geq 1.0 \quad (23)$$

where β_P is the ratio of design dead load to design total load

ρ_t is the total reinforcement ratio
 $= (A_s + A'_s)/A_c$

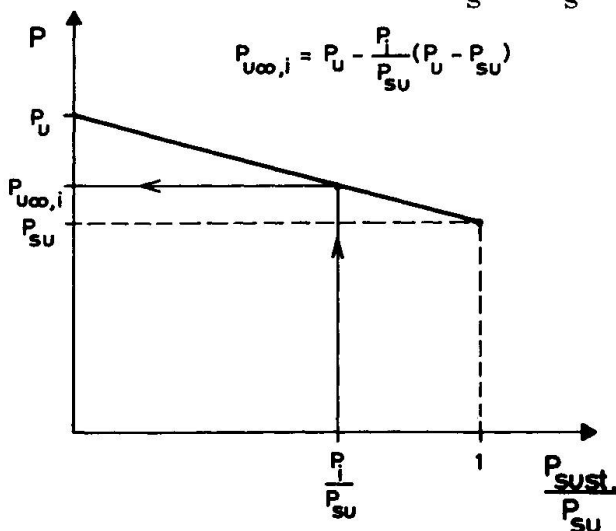


FIG. 8: REDUCED ULTIMATE LOAD CAPACITY DUE TO SUSTAINED LOAD (APPROXIMATION)

As pointed out in 5.1, columns subjected to high sustained loads may fail under the sustained load. In order to find the critical ultimate sustained load, P_{su} , the creep parameter β_s had to be derived from the value P_{su} found in the computer tests. β_s was derived in the same manner as β except that $P_{u\infty,i}$ and $M_{u\infty,i}$ had to be replaced by P_{su} and M_{su} . For M_{su} , the moment on interaction curve (\bar{A}) (Fig. 7) at the level of P_{su} was chosen because (\bar{A}) is the only interaction curve available to the designer and therefore the use of M_{su} from curve (\bar{D})

would have led to creep parameters which would overestimate P_{su} . Eqn. (24) represents a simplified regression equation for design use:

$$\beta_s = 0.06 \quad l/h \geq 1.0 \quad (24)$$

In the procedure considered, the column would first be proportioned for the design (ultimate) load using Eqns. (19, 21 and 23). The check whether the column would fail during the sustained load period would then be carried out using Eqns. (19, 21 and 24) with $\beta = \beta_s$ in Eqn. (19).

The Reduced E-Modulus Method is well suited to be used in the simplified step-by-step analysis procedure discussed in 4.1. The critical sustained load capacity, P_{su} , may be computed exactly in the same manner as the ultimate load capacity P_u replacing E_c by the reduced modulus $E_c(t=\infty)$ computed from Eqn. (25)

$$E_c(t) = \frac{E_c}{1 + \varphi(t)} \quad (25)$$

The creep coefficient $\varphi_\infty = \varphi(t=\infty)$ follows from Eqn. (15) inserting $t=\infty$ and assuming an average ratio $f_c/f'_c = 0.40$. For the computation of the internal forces the diagrams in Fig. 4 can be used again but prior to the evaluation of k_c and k_y the assumed strain distribution has to be divided by $(1 + \varphi_\infty)$. The ultimate concrete strain under sustained loads, ϵ_{su} , has been limited to $(1 + \varphi_\infty)$ times the instantaneous strain given by Eqn. (14) on the stress level $f_c/f'_c = 0.88$. The strength of concrete has been assumed in the computation as 80 % of the short time strength of concrete of the same age. Since the short time strength at time infinity has been assumed equal to $1.10 f'_{c28}$, the critical sustained stress will be $0.8 \cdot 1.10 f'_{c28} = 0.88 f'_{c28}$. The assumed ultimate strain

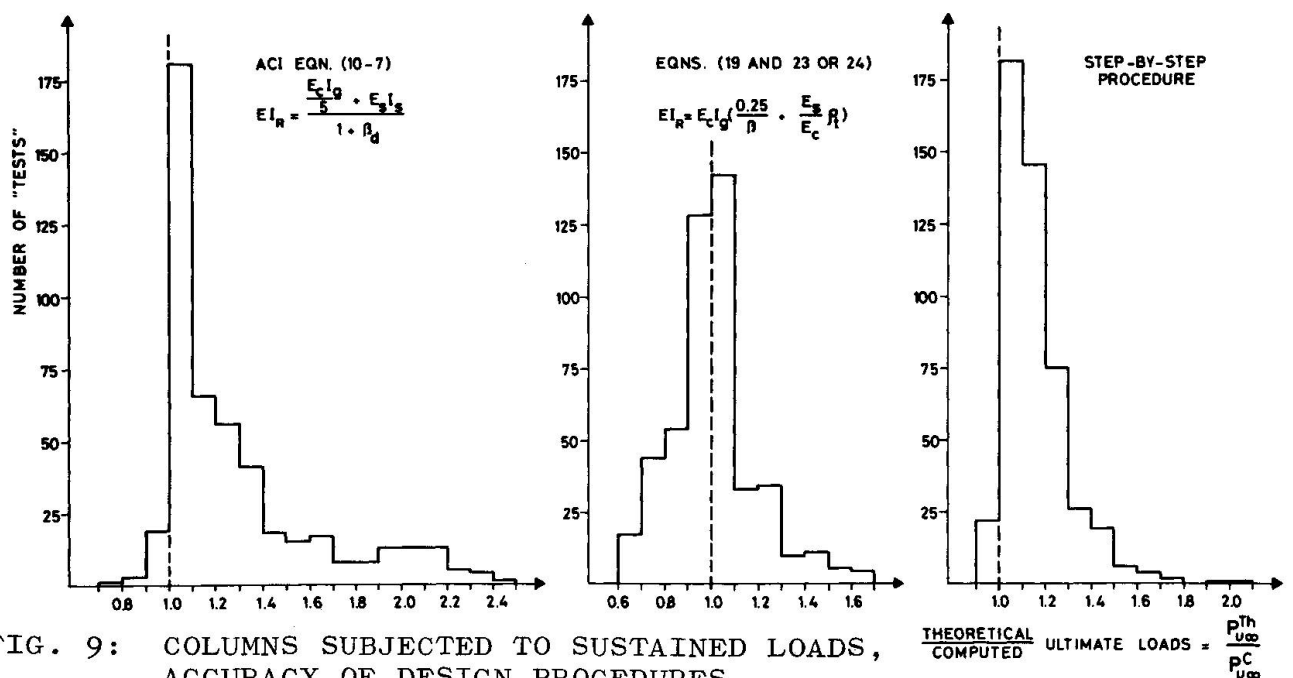


FIG. 9: COLUMNS SUBJECTED TO SUSTAINED LOADS, ACCURACY OF DESIGN PROCEDURES

TABLE 8
COMPARISON OF DESIGN PROCEDURES
WITH COMPUTER EXPERIMENTS
(Columns Subjected to Sustained Loads)

Design Method (Total Sample- 482 Columns)	Ratio of $P_{u\infty}^{Th}/P_{u\infty}^C$	
	Mean	Coef. of Var. %
Reduced E-Modulus Concept used in Moment Magnifier Method Ref.(3)		
ACI Eqn.(10-7)	1.290	26.4
ACI Eqn.(10-8)	1.373	33.6
Eqn.(19 and 23 or 24)	1.013	17.9
Eqn.(20 and 23 or 24)	1.045	20.3
Dischinger Method(Ref.(3))	1.063	16.5
Magnified Eccentricity Method Ref.(3)	1.109	16.8
Creep Eccentricity Method Ref.(3)		
CEB Version	1.568	30.0
Version proposed in Ref.(3)	1.115	17.6
Reduced E-Modulus Concept used in Step-by-Step Analysis Procedure	1.156	12.1

was reached by four columns only. Moreover, this limitation of the strain appears to be of minor importance because P_{su} increased by not more than 0.35 % for an unlimited stress-strain curve.

P_u represents an upper bound on the ultimate load capacity and P_{su} represents a lower bound (Fig. 7). An increase of the sustained load portion results in a gradual decrease of the ultimate load capacity from P_u to P_{su} . As a simplification for design it has been assumed that the ultimate load decreases proportionally to the increase of the sustained load portion as shown in Fig. 8. This assumption is slightly over-conservative.

In the Step-by-Step Design Method it is advisable to compute P_{su} first if the sustained load

portion is considerable. If the check shows that there is no danger of a creep failure, P_u is computed and the ultimate load capacity for the total design load is found by linear interpolation between P_u and P_{su} as shown in Fig. 8.

Table 8 shows the accuracy of different design procedures in the case of the computer experiment including 482 columns. The design methods proposed in Ref. 3 are clearly more accurate than the 1971 ACI Method. However, neither the Dischinger Method nor the Creep Eccentricity Method was found to be superior to the Reduced E-Modulus Method. Compared to all the methods considered the Step-by-Step Method described in this paper is clearly the most accurate procedure as shown by Table 8 and Fig. 9. In addition, less values are on the unsafe side ($P_{u\infty}^{Th}/P_{u\infty}^C < 1.0$) as shown by Fig. 9.

As for short-term tests a comparison between design procedures and tests on reinforced concrete columns investigated by several authors (Refs. 15, 17, 18, 19, 20) has been carried out. The usual

TABLE 9
COMPARISON OF DESIGN METHODS WITH SUSTAINED LOAD COLUMN TESTS

Design Method (Total Number of Tests - 53 Columns)	Ratio of $P_{u(t)}^{Test}/P_{u(t)}^C$		Investigators and Number of Tests*
	Mean	Coef. of Var. %	
Reduced E-Modulus Concept used in Moment Magnifier Method			Thürlimann, Ref.(17), N = 12 Kordina, Ref.(20), N = 12 Goyal, Jackson, Ref.(19), N = 20 Gaede (Diamond), Ref.(15), N = 1 Drysdale, Huggins (Diamond), Ref.(18) N = 8
ACI Eqn.(10-7)	1.278	20.5	
Eqn.(19 and 23 or 24)	0.997	18.7	
Reduced E-Modulus Concept used in Step-by-Step Analysis Procedure	1.069	12.8	*) The investigation includes columns which failed in a final short-term test after a period of sustained loading. Columns which failed under sustained load (Refs.(15,17,18)) have been excluded.

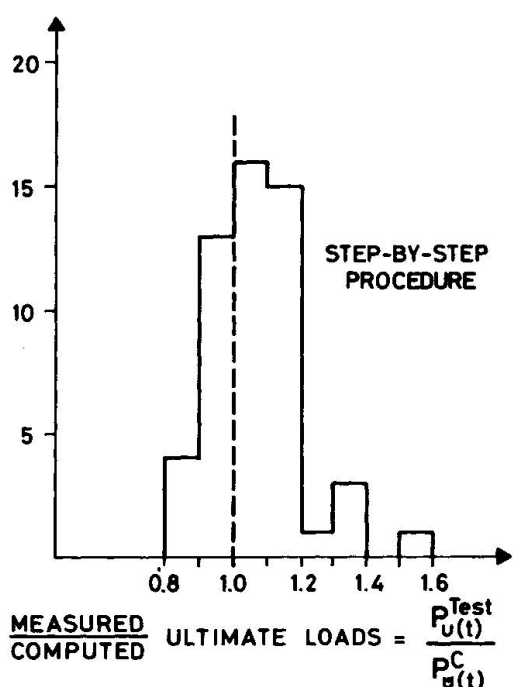
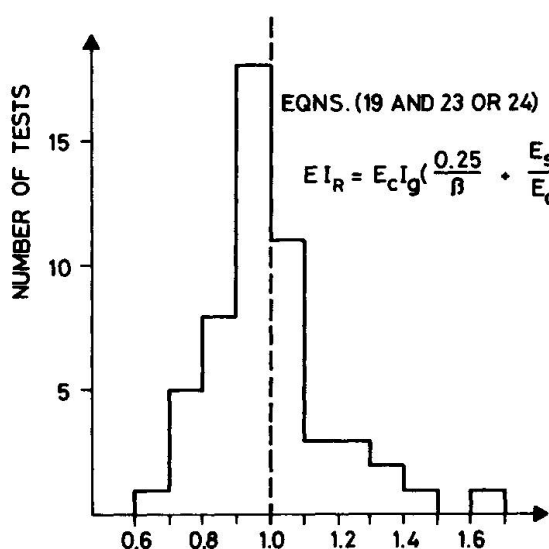


FIG. 10: COMPARISON OF DESIGN PROCEDURES WITH SUSTAINED LOAD COLUMN TESTS

as they will usually not lead to an appreciable increase of the total structural costs (30). Sophisticated computer oriented incremental analysis procedures such as described in sections 2.1 and 5.2 are therefore not suited to be used in common design practice.

The comparisons of approximate column design methods with computer analyses and column tests presented in this paper confirm that the simplest methods also prove to be the least accurate (6) and in a few cases the prediction of the ultimate load capacity is found to be considerably unsafe.

The general trend to make use of programmable desk calculators in design practice allows the development of simple step-by-step

test procedure is to subject a column to a constant sustained load; if no creep failure occurs within a certain time period the column is loaded up to failure in a final short-term test. To compute the ultimate load of these columns the time dependent development of the creep parameter was taken as $\gamma(t)$ times the values at $t=\infty$, where:

$$\gamma(t) = 1 - \exp(-0.1325 \sqrt{t}) \quad (26)$$

Columns which failed under sustained load have not been considered in this investigation. The ratio between measured and computed ultimate loads is shown by histograms in Fig. 10 for 53 sustained load column tests. The characteristic values of the distributions including the 1971 ACI Method, the improved Moment Magnifier Method from Ref. 3 and the Step-by-Step Method are shown in Table 9. Considering the coefficient of variation the ACI Method is poorer than the method based on Eqns. (19 and 23 or 24) but both methods gave much poorer prediction than the Step-by-Step Method (Table 9).

6. CONCLUDING REMARKS

Economically the columns account in most cases for a rather small part of the total structural costs but structurally they constitute a vital part of the structure (Ref. 30). As a consequence relatively simple and conservative design procedures are preferable

analysis procedures for design purposes. Compared to moment magnifier method or complementary eccentricity method (31) the step-by-step analysis method provides more accurate predictions of the behavior and load carrying capacity of concrete columns. The application of the method to columns which are components of frames or structural subassemblages needs further research.

REFERENCES

1. ACI Committee 318, "Building Code Requirements for Reinforced Concrete (ACI 318-71)", American Concrete Institute, Detroit, 1971.
2. MacGregor, J.G., Oelhafen, U.H. and Hage, S., "A Re-examination of the EI Value for Slender Columns", Reinforced Concrete Columns, Special Publication, American Concrete Institute (in Press - 1974)
3. Oelhafen, U.H. and MacGregor, J.G., "The Design of Slender Columns Subjected to Sustained Loads", Reinforced Concrete Columns, Special Publication, American Concrete Institute (in Press - 1974)
4. Oelhafen, U.H., "Formänderungen von Stahlbetonstützen unter exzentrischer Druckkraft", Institut für Baustatik, ETH, Bericht No. 31, Zürich, 1970.
5. Fisher, R.A., "The Design of Experiments", Hafner Publishing Company, New York, 1960.
6. Warner, R.F., "Physical-Mathematical Models and Theoretical Considerations", Theme Paper I, Preliminary Report, IABSE-CSCE Symposium on Design and Safety of Reinforced Concrete Compression Members, Zürich, 1973.
7. MacGregor, J.G., Breen, J.E., Pfrang, E.O., "Design of Slender Concrete Columns", ACI Journal, Proceedings Vol. 67, No. 1, January 1970.
8. Baumann, O., "Die Knickung der Eisenbeton-Säulen", Eidg. Materialprüfungsanstalt an der ETH, Zürich, Bericht No. 89, Zürich, 1934.
9. Thomas, F.G., "Studies in Reinforced Concrete VII. Strength of Long Reinforced Concrete Columns in Short Period Tests to Destructions", Department of Scientific and Industrial Research, Building Research Technical Paper No. 24, London, 1939.
10. Hanson, R. and Rosenstrøm, S., "Trykkforsøk med slanka betongpelare", Betong, Vol. 32, No. 3, Stockholm, 1947.
11. Rambøll, B.J., "Reinforced Concrete Columns", Teknisk forlag, Copenhagen, 1951.
12. Ernst, G.C., Hromadik, J.J., Riveland, A.R., "Inelastic Buckling of Plain and Reinforced Concrete Columns, Plates and Shells", University of Nebraska Engineering Experiment Station Bulletin No. 3, Lincoln, Nebraska, 1953.
13. Gaede, K., "Knicken von Stahlbetonstäben unter Kurz- und Langzeitbelastung", Deutscher Ausschuss für Stahlbeton, Heft No. 129, Berlin, 1958.
14. Chang, W.F. and Ferguson, P.M., "Long Hinged Reinforced Concrete Columns", ACI Journal, Proceedings Vol. 60, No. 1, January 1963.
15. Gaede, K., "Knicken von Stahlbetonstäben mit quadratischem Querschnitt in Richtung einer Diagonalen unter Kurz- und Langzeitbelastung", Institut für Materialprüfung u. Forschung des Bauwesens, Universität Hannover, 1968.

16. Robinson, J.R. and Modjabi, S.S., "La Prévision des Charges de Flambement des Poteaux en Béton Armé par la Méthode de M.P. Faessel", Annales de l'Institut Technique du Bâtiment et des Travaux Publics, No. 249, Paris, September 1968.
17. Ramu, P., Grenacher, M., Baumann, M., Thürlimann, B., "Versuche an gelenkig gelagerten Stahlbetonstützen unter Dauerlast", Institut für Baustatik, ETH, Bericht No. 6418-1, Zürich 1969.
18. Drysdale, R.G., Huggins, M.W., "Sustained Biaxial Load on Slender Concrete Columns", Journal of the Structural Division, ASCE, Vol. 97, ST5, May 1971.
19. Goyal, B.B., Jackson, N., "Slender Concrete Columns Under Sustained Load", Journal of the Structural Division, ASCE, Vol. 97, ST11, November 1971.
20. Kordina, K., "Langzeitversuche an Stahlbetonstützen", Deutscher Ausschuss für Stahlbeton, (in press)
21. Kukulski, W. and Lewicki, B., "Contribution to the Discussion about the Simplified Calculations Methods for Eccentrically Loaded Columns", Memorandum to CEB Commission 8, Flambement, Warsaw, September 1969. (This memorandum summarizes the results of tests by Tal and Chistia-kov).
22. Mehmehl, A., Schwarz, H., Kasperek, K.H., Makovi, J., "Tragverhalten ausmittig beanspruchter Stahlbetondruckglieder", Deutscher Ausschuss für Stahlbeton, Heft No. 204, Berlin, 1969.
23. Mauch, S.P. and Holley, M.J., "Creep Buckling of Reinforced Concrete Columns", Journal of the Structural Division, Vol. 89, ST4, August 1963.
24. Manuel, R.F. and MacGregor, J.G., "Analysis of Restrained Reinforced Concrete Columns Under Sustained Load", ACI Journal, Proceedings Vol. 64, No. 1, January 1967.
25. Comité Européen du Béton, "CEB-FIP International Recommendations for the Design and Construction of Concrete Structures", FIP Sixth Congress, Prague, June 1970.
26. Rüsch, H., "Researches Toward a General Flexural Theory for Structural Concrete", ACI Journal, Proceedings Vol. 57, No. 1, July 1960.
27. Dischinger, F., "Untersuchungen über die Knicksicherheit, die elastische Verformung und das Kriechen des Betons bei Bogenbrücken", Bauingenieur, Vol. 18 and 20, Berlin 1937 and 1939.
28. MacGregor, J.G., "Simple Design Procedures for Concrete Columns", Theme Paper II, Preliminary Report, IABSE-CSCE Symposium on Design and Safety of Reinforced Concrete Compression Members, Zürich, 1973.
29. Commission 8, "Manuel de Calcul CEB-FIP, Buckling-Instability", Bulletin d'Information No. 79, Comité Européen du Béton, Paris, Jan. 1972.
30. Thürlimann, B., Summary Report, Technical Committee No. 21, Elastic Analysis-Strength of Members and Connections, Volume III, IABSE-ASCE Joint Committee on Planning and Design of Tall Buildings, ASCE, New York, 1972.
31. Cranston, W.B., "Analysis and Design of Reinforced Concrete Columns", Research Report 20, Cement and Concrete Association, 41.020, London, 1972.

SUMMARY

The accuracy of simple design procedures for concrete columns under short-term and sustained loads is investigated. Statistical comparisons of design method with computer analyses and column tests show limited improvement capacity of the common Moment Magnifier Method (ACI Code 318-71). However, a design procedure based on a step-by-step analysis of the load-moment relationship of the column takes proper account of material failure and stability failure; therefore it is considerably more accurate.

RESUME

On étudie la précision des méthodes simples de dimensionnement des colonnes en béton soumises à des sollicitations instantanées ou de longue durée. On effectue des comparaisons statistiques avec des calculs d'ordinateur et des résultats d'essais: il s'avère qu'on ne peut guère améliorer la méthode des "Moment Magnifier" (ACI 318-71). Un procédé qui permet un calcul pas-à-pas de la courbe charge-moment de la colonne s'avère par contre plus précis, car il tient exactement compte des processus de rupture, qu'il soient dûs ou non au flambement.

ZUSAMMENFASSUNG

Die Zuverlässigkeit einfacher Berechnungsverfahren für Betonstützen unter Kurz- und Langzeitbeanspruchung wird untersucht. Statistische Vergleiche mit Computerberechnungen und Stützenversuchen zeigen eine beschränkte Verbesserungsfähigkeit der bekannten "Moment Magnifier"-Methode (ACI Code 318-71). Ein Verfahren, bei dem die Last-Moment-Kurve der Stütze schrittweise berechnet wird, erweist sich dagegen als bedeutend zuverlässiger, da dieses Verfahren sowohl den Festigkeits- als auch den Stabilitätsbruch qualitativ richtig erfasst.

Leere Seite
Blank page
Page vide